Electrochemistry of Spontaneously Adsorbed Monolayers. Equilibrium Properties and Fundamental Electron Transfer Characteristics

Robert J. Forster and Larry R. Faulkner*

Contribution from the Department of Chemistry, University of Illinois, 600 S. Mathews Avenue, Urbana, Illinois 61801

Received November 29, 1993®

Abstract: The effects of solvent, electrolyte, and temperature on the electrochemical response of spontaneously adsorbed monolayers of $[Os(bpy)_2Cl(pNp)]^+$, where bpy is 2,2′-bipyridyl and p*N*p is 4,4′-bipyridyl, 1,2-bis(4-pyridyl)ethane, or 4,4′-trimethylenedipyridine, are examined. In tetrahydrofuran oxidation of the redox centers causes association of an extra anion, while two extra anions are bound to the oxidized centers in aqueous media. In aqueous solutions containing hydrophilic anions, such as nitrate or chloride, little ion pairing is observed. The temperature dependence of the formal potential over the range −5 to 40 °C shows that the reaction entropy ($\Delta S_{rc}°$) is positive, indicating increased solvent ordering in the higher oxidation state. A linear correlation is observed between the experimental reaction entropies and those predicted by the Born dielectric continuum model in a range of solvents. A non-adsorbing model compound, $[Os(bpy)_2(pyridine)Cl]PF_6$, typically exhibits considerably smaller $\Delta S_{rc}°$ values, suggesting that the formation of a dense monolayer significantly affects the reaction entropy. The heterogeneous rate constant k for the $Os^{2+/3+}$ reaction has been evaluated using nanosecond time scale chronoamperometry. Importantly, k is approximately independent of the supporting electrolyte concentration over the range 0.1 to 1.0 M. This may suggest that ion pairing is an equilibrium reaction that either precedes or follows electron transfer. Tafel plots of the dependence of ln k on overpotential show curvature, indicating that the transfer coefficient is potential dependent. For sufficiently large overpotentials k tends to become independent of the free energy driving force, which is consistent with Marcus theory. The response is asymmetric with respect to overpotential, with the slope for the oxidation process tending toward zero more rapidly than that for the reduction process. This response can be modeled as a tunneling process between electronic manifolds on the two sides of the interface.

Introduction

The redox properties of electroactive centers within organized monolayers and the characteristics of the modified interface have received renewed interest in recent years.[1-4] This is because adsorbed monolayers enable both the nature of the chemical functional groups and their topology to be controlled, thus allowing the effects of both chemical and geometric properties on the overall electron transfer rate to be explored.[5,6]

In this paper, and its following companion, we report on the ionic interactions and heterogeneous electron transfer kinetics within a family of spontaneously adsorbed monolayers that seem extraordinarily well behaved. The heterogeneous electron transfer reaction of interest involves the $Os^{2+/3+}$ redox reaction within monolayers of $[Os(bpy)_2Cl(pNp)]^+$ (Chart 1), where bpy is 2,2′-bipyridyl and p*N*p is either 4,4′-bipyridyl, 1,2-bis(4-pyridyl)-ethane, or 4,4′-trimethylenedipyridine. Since the bridging ligand between the redox center and the electrode contains zero, two, or three methylene spacer groups between the two pyridyl rings, we denote the monolayers simply as p0p, p2p, and p3p, respectively. The practically ideal electrochemical responses of these monolayers have enabled us to make an unprecedented range of measurements on the individual systems. We have investigated the electrochemical response as a function of electrolyte, solvent, temperature, and electron transfer distance. It is only with such well-behaved experimental systems that fundamental issues such as the dependence of the heterogeneous electron transfer rate on the reaction free energy, the electron transfer distance, the molecular structure of the interface, or indeed the solvent can be meaningfully addressed. These investigations have been fruitful, not only in identifying the effects of these variables on the heterogeneous kinetics but also in revealing possible deficiencies in existing models of electron transfer.

Chart 1

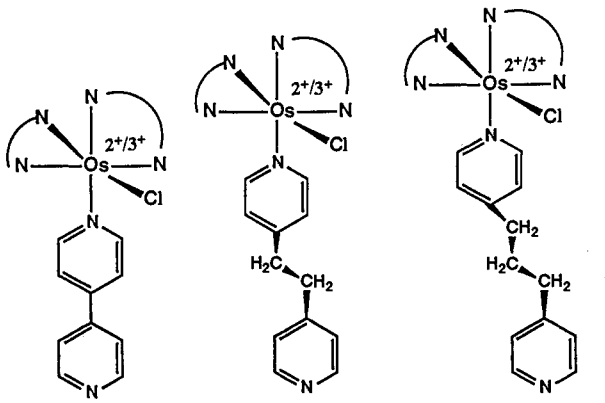

In this first paper, we probe the local microenvironment of the redox centers by investigating the way in which the thermodynamic aspects of the electrochemical response depend on the supporting electrolyte, solvent, and temperature. These results are important, because an insight into the monolayer structure is essential in understanding those factors that influence heterogeneous kinetics, which is the topic of ultimate interest in this pair of papers. For electroactive monolayers, redox reactions alter the charge density within the monolayer giving the possibility of changing ionic

* Author to whom correspondence should be addressed.
* Abstract published in *Advance ACS Abstracts*, May 15, 1994.

(1) Chidsey, C. E. D.; Loiacono, D. N. *Langmuir* **1990**, *6*, 682.
(2) Finklea, H. O.; Snider, D. A.; Fedik, J. *Langmuir* **1990**, *6*, 371.
(3) Strong, L.; Whitesides, G. M. *Langmuir* **1988**, *4*, 546.
(4) Nuzzo, R. G.; Dubois, L. H.; Allara, D. L. *J. Am. Chem. Soc.* **1990**, *112*, 558.
(5) Nordyke, L. L.; Buttry, D. A. *Langmuir* **1991**, *7*, 380.
(6) Li, T. T.-T.; Weaver, M. J. *J. Am. Chem. Soc.* **1984**, *106*, 6107.

0002-7863/94/1516-5444$04.50/0

interactions,[7] which may influence the electron transfer kinetics. Furthermore, the rational and predictable manipulation of surface functionality by immobilization of surfactants requires an understanding of molecular interactions within assemblies. Redox centers incorporated within self-organized films are particularly effective probes of the local microenvironment, since the formal potential is sensitive to its physicochemical surroundings. In particular, we find that for these monolayers the extent of ion pairing between the oxidized redox center and an anion depends on not only the anion's identity and concentration but also the electrochemical solvent. Immobilization within a dense monolayer is likely to affect the solvation shell of an electroactive center. We have quantified the extent of solvent ordering from temperature-resolved measurements of the formal potential. The difference in solvent ordering between the reduced and oxidized forms of the redox couple is considerably larger for the surface-confined redox center compared to a solution analog. Furthermore, greater solvent ordering occurs for the shorter bridging ligand, suggesting that interactions of solvent dipoles with the electric field may contribute significantly to the observed entropy.

The kinetic behavior has been studied via chronoamperometry, which is remarkably well-behaved over a wide range of time scales, temperatures, and solvents. This ideality makes these molecular ensembles attractive for investigating the role of overpotential and temperature in determining heterogeneous electron transfer rates. In this work we formed spontaneously adsorbed monolayers on microelectrodes to avoid diffusive limitations on the microsecond electron transfer kinetics. The use of microelectrodes also allows the dependence of the interfacial kinetics on driving force to be explored over a large potential range. The dependence of the rate constant on potential is consistent, in all details, with a model involving tunneling between electronic manifolds on the two sides of the interface.

In the second paper,[8] we present a much more detailed investigation of the kinetics of heterogeneous electron transfer. The ideal chronoamperometric response and the thermal stability of the monolayers make them ideal model systems for investigating the predictive ability of existing electron transfer models. The ability of the Butler–Volmer formulation to accurately model the potential and temperature dependence of the electrode kinetics receives special attention in our companion paper. We also report on the influence of solvent in determining electron transfer rates. This detailed analysis has allowed the influence of the solvent on the activation barrier, and the effect of solvent dynamics on the interfacial kinetics, to be determined.

The combined results from both papers are extremely revealing of the molecular and ionic interactions that occur within dense monolayers and their influence on the electron transfer kinetics.

Experimental Section

$[Os(bpy)_2Cl_2]$ was prepared by a modification of the procedure described by Buckingham et al.[9] using $OsCl_3$ as the starting material instead of $K_2[OsCl_6]$. Surface active osmium complexes were synthesized by refluxing $[Os(bpy)_2Cl_2]$ with a 2- to 3-fold excess of the appropriate bridging ligand in methanol for several hours. In a typical synthesis, 200 mg of $[Os(bpy)_2Cl_2]$ (0.35 mmol) was placed in 50 cm^3 of methanol and refluxed for 10–20 min to ensure complete dissolution of the complex. A solution of 130 mg of 1,2-bis(4-pyridyl)ethane (Aldrich) (0.70 mmol) in 10 cm^3 of methanol was added, after which time refluxing was continued for an additional 8 h. Excess solvent was removed by rotary evaporation and, following cooling to room temperature, a 3-fold molar excess of NH_4PF_6 dissolved in 5 cm^3 of H_2O was added to precipitate $[Os(bpy)_2Cl(p2p)]PF_6$. The product was filtered and washed with ice water and ether. The complex was recrystallized from aqueous methanol to give red-brown crystals, yield 260 mg, 86%.

Microelectrodes were fabricated from platinum wires (Goodfellow Metals Ltd.) of radii between 1 and 25 μm by sealing them in soft glass using a procedure described previously.[10] The microdisk electrodes were exposed by removing excess glass using 600 grit emergy paper followed by successive polishing with 12.5-, 5-, 1-, 0.3-, and 0.05-μm alumina. The electrodes were then electrochemically cleaned in 0.1 M $HClO_4$ by cycling between potential limits chosen to initially oxidize and subsequently to reduce the surface of the platinum electrode. The potential was then held in the double layer region for 100 s at a sufficiently negative value to ensure complete reduction of any surface oxide. Finally, the electrode was cycled between –0.3 and 0.7 V in 0.1 M $NaClO_4$ until hydrogen desorption was complete. The area of these electrodes was determined from cyclic voltammetry and chronocoulometry using $[Os(bpy)_3]^{2+}$ as an electrochemical probe. This area corresponded, within 5–10%, to the geometric area anticipated for a disk, confirming the observation made using an optical microscope that the sealing and polishing procedure results in a disk-shaped electrode. The electrochemically active, or microscopic, area of the prepared electrodes was determined from both oxide reduction and hydrogen adsorption–desorption measurements in 0.1 M $HClO_4$.[11] The surface roughness factors were typically between 1.6 and 2.0. RC cell time constants were in the range of 30 to 300 ns depending on the electrode radius and the electrolyte system. The interfacial kinetics were measured only at times greater than about 5–10 RC.

Spontaneously adsorbed monolayers were typically formed by immersing the electrodes in a 10 mM solution of the metal complex in either 50:50 aqueous dimethylformamide or 50:50 aqueous acetone for several minutes. Before electrochemical measurements, the modified electrodes were rinsed with the electrochemical solvent to remove unbound material. Subsequent measurements were performed in blank electrolyte solutions.

Electrochemical cells were of conventional design and were thermostated within ±0.2 °C using a PolyScience Model 9510 refrigerating circulator. All potentials are quoted with respect to a BAS Ag/AgCl gel-filled reference electrode, the potential of which was 37 mV more positive than the saturated calomel electrode (SCE). A non-isothermal cell, where the reference electrode was isolated from the main compartment by a salt bridge and held at room temperature, was used for the investigation of temperature effects on the formal potential, $E^{\circ\prime}$. The non-isothermal salt bridge typically contained 3.0 M aqueous KCl since it has a low resistance, and the salt remains soluble at the lowest temperature employed (–5 °C). This high concentration and the design of the bridge should minimize any systematic error in the reported temperature effects on $E^{\circ\prime}$ due to changes in the liquid junction potential with temperature.[12] Similar shifts in the formal potential with temperature were observed when the non-isothermal salt bridge contained the same supporting electrolyte as the main cell compartment, although the total cell resistance was somewhat higher. Cyclic voltammetry at the microelectrodes was performed using a BAS-100B electrochemical analyzer and a PA-1 low-current preamplifier. The electrochemical cell was housed in a Faraday cage during cyclic voltammetry. A custom-built programmable function generator–potentiostat, which had a rise time of less than 10 ns, was used to apply potential steps of variable pulse width and amplitude directly to the two-electrode cell. A Pt foil and an Ag/AgCl reference electrode were combined to form a counter electrode. The foil lowered the resistance and provided a high-frequency path. The current-to-voltage converter was based on a Comlinear CLC 203 AI operational amplifier with a 1500 Ω feedback resistance and a response time of less than 10 ns. The chronoamperograms were recorded using a HP54201A digital oscilloscope in the 64X time-average mode. First-order rate constants were extracted from the slope of ln $i(t)$ vs t plots using software routines written in Microsoft QuickBASIC. All solutions were thoroughly degassed using nitrogen, and a nitrogen blanket was maintained over the solution throughout the experiments. Solvents were typically spectrometric or HPLC grade and they were dried and purified using standard laboratory procedures.[13] Acetonitrile (Aldrich, HPLC grade, water content below 0.02%) was dried over 4A molecular sieves. Acetone (Fisher Chemicals) was dried using potassium carbonate followed by vacuum distillation. DMF (Aldrich, HPLC grade, water content below 0.03%) was dried over 4A molecular sieves. Tetrahydrofuran (EM Science) was dried using potassium hydroxide. Dichloroethane (EM Science) was vacuum distilled over sodium sulfate. Chloroform was

(7) DeLong, H. C.; Donohue, J. J.; Buttry, D. A. *Langmuir* **1991**, *7*, 2196.
(8) Forster, R. J.; Faulkner, L. R. *J. Am. Chem. Soc.* following paper in this issue.
(9) Buckingham, D. A.; Dwyer, F. P.; Goodwin, H. A.; Sargeson, A. M. *Aust. J. Chem.* **1964**, *17*, 325.
(10) (a) Faulkner, L. R.; Walsh, M. R.; Xu, C. *Contemporary Electroanalytical Chemistry*; Ivaska, A., Ed.; Plenum Press: New York, 1990; p 5. (b) Xu, C. Ph.D. Thesis, University of Illinois at Urbana—Champaign, 1992.
(11) Trasatti, S.; Petrii, O. A. *J. Electroanal. Chem.* **1992**, *327*, 354.
(12) Yee, E. L.; Cave, R. J.; Guyer, K. L.; Tyma, P. D.; Weaver, M. J. *J. Am. Chem. Soc.* **1979**, *101*, 1131.
(13) Riddick, J. A.; Bunger, W. B. *Organic Solvents*; Weissberger, A., Ed.; Wiley: New York, 1970.

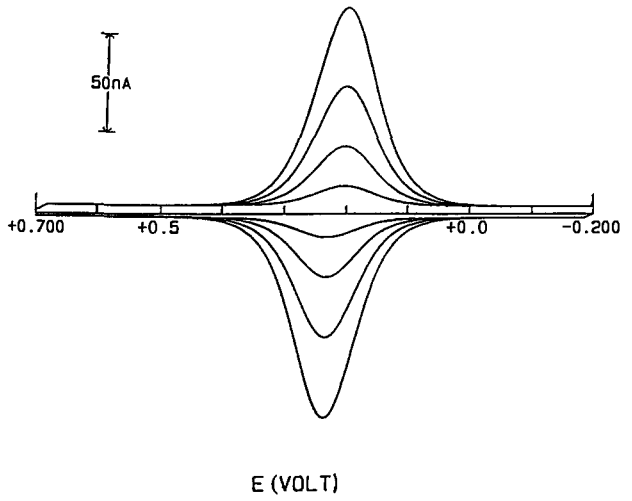

Figure 1. Scan rate dependence of the cyclic voltammograms for a spontaneously adsorbed p2p monolayer. The scan rates are (top to bottom) 50, 30, 15, and 5 V/s. The surface coverage is 7.7×10^{-11} mol cm^{-2}. The supporting electrolyte is aqueous 0.1 M $NaClO_4$. The radius of the Pt microelectrode is 25 μm. The cathodic currents are up, and the anodic currents are down. Each cycle begins at the negative limit.

washed with concentrated sulfuric acid to remove the ethanol preservative (0.75%), then it was washed with 0.1 M sodium hydroxide and then with ice water. It was then dried over potassium carbonate and distilled under vacuum shortly before use. All solvents were stored over activated 4A molecular sieves. These procedures are expected to reduce the water content to low millimolar concentrations.

Results and Discussion

General Information. Figure 1 shows a typical cyclic voltammogram for a spontaneously adsorbed p2p monolayer, where the supporting electrolyte is aqueous 0.1 M $NaClO_4$. The peak shape is independent of scan rate up to 50 V/s, and the peak height scales linearly with scan rate. For all solvents investigated, repetitive cycling over a 4-h period at temperatures up to 40 °C does not change the voltammograms, demonstrating that these monolayers are stable to electrochemical cycling.

The potentials at which the anodic and cathodic current maxima are observed are typically separated by less than 35 mV, and the full width at half maximum (fwhm) is 90–110 mV. Where there are no lateral interactions between surface confined redox centers and a rapid equilibrium is established with the electrode, a zero peak-to-peak splitting (ΔE_P) and an fwhm of 90.6 mV are expected for a one-electron transfer.[14] Our observation that ΔE_P is simultaneously nonzero, and independent of scan rate ν, suggests that slow charge-transfer kinetics are not the origin of the observed response. Slow kinetics would cause ΔE_P to increase with increasing scan rate. Ohmic effects are not an explanation for the finite, scan rate independent ΔE_P, since a larger iR drop would be expected at higher scan rates because of the larger total current passed. Furthermore, diffusion is effectively excluded as an explanation since the peak height increases linearly with scan rate, rather than the $\nu^{1/2}$ dependence expected for a diffusing species. There have been previous reports of finite ΔE_P values for surface confined redox couples that are independent of scan rate, including ferrocene carboxylic acids on platinum[15] and $[Ru(bpy)_3]^{2+}$ electrostatically bound within Nafion.[16] Feldberg and Rubinstein have interpreted this unusual quasireversibility (UQR), or apparent nonkinetic hysteresis in cyclic voltammetry, in terms of N-shaped free energy curves.[17] In their interpretation, hysteretic UQR behavior is a non-equilibrium behavior arising because some rate processes are slow on the time scale of the experiment, thus causing a finite ΔE_P to be observed.

For those solvents in which the model compound, $[Os(bpy)_2(pyridine)Cl]^+$, is soluble, we observe only 10–20-mV differences between the formal potentials ($E^{\circ\prime}$) of the solution-phase model complex and the monolayer. This is consistent with the redox centers residing in the solution phase outside the aromatic and alkane anchor of the monolayer. Changing the electron transfer distance by altering the number of methylene spacer groups in the bridging ligand results in very similar cyclic voltammograms to those illustrated in Figure 1, with the same $E^{\circ\prime}$ values being observed for the three modified electrodes to within 25 mV.

After correcting for the background charging current, the total charge withdrawn or injected to oxidize or reduce the monolayer can be determined from the area under the voltammetric peak. From this charge and the microscopic electrode area, the surface coverage (the number of moles of $[Os(bpy)_2Cl(p2p)]^+$ per cm^2) can be determined. This provides important information about the packing density of the monolayer. The surface coverage Γ is $7.7 \pm 0.15 \times 10^{-11}$ mol cm^{-2}, which gives an area per molecule of approximately 240 Å^2, based on the microscopic surface area. Crystallographic data for related osmium polypyridyl complexes[18] suggest that the radius of the osmium complex considered here is approximately 7.5 Å, giving a projected area per molecule of around 180 Å^2. When additional contributions to molecular volume are considered (e.g., that of a solvent shell or a counterion), it appears that adsorption produces nearly a complete monolayer.

While Figure 1 is specific for a p2p monolayer, the results are also representative of the behaviors observed for the p0p and p3p monolayers. In the following discussions, unless stated otherwise, we illustrate behavior that is qualitatively the same for all three monolayers using data for a single type of monolayer.

Interfacial Capacitance. One expects that immobilization of a monolayer at the electrode/solution interface would alter the double layer structure, and change the effective dielectric constant.[19,20] Therefore, one expects the double layer capacitance to be sensitive to the chemical composition of the monolayer and the packing density. We have determined the interfacial capacitance as a function of potential, and hence oxidation state of the monolayer, using small amplitude potential step chronoamperometry. In these experiments the potential was stepped from an initial value E_i using a pulse amplitude of 50 mV, and the resulting current response was recorded. In successive measurements, E_i was increased monotonically by 50 mV from –0.200 to 0.600 V. Stepping the potential in a region where the redox composition of the monolayer did not change, i.e., far from $E^{\circ\prime}$, gave only a single exponential current decay due to double layer charging. When the potential was stepped in a region close to $E^{\circ\prime}$, we observed two time-resolved first-order decays, corresponding to double layer charging and the Faradaic reaction, respectively. In both cases the capacitive current arising from double layer charging was analyzed using a plot of ln $i(t)$ vs t. The resistance R_u and integral double layer capacitance C_{dl} were determined using eq 1:[21]

$$i_c(t) = (\Delta E/R_u) \exp(-t/R_u C_{dl}) \qquad (1)$$

where ΔE is the pulse amplitude. In plotting these data, we associate each value of C_{dl} with the initial potential E_i of the experiment used to obtain it. Figure 2 shows the interfacial capacitance and redox composition, determined from chronocoulometry, as a function of potential for a spontaneously adsorbed p3p monolayer in aqueous 0.1 M $NaClO_4$. The double layer

(14) (a) Laviron, E. *J. Electroanal. Chem.* **1974**, *52*, 395. (b) Brown, A. P.; Anson, F. C. *Anal. Chem.* **1977**, *49*, 1589.
(15) Lenhard, J. R.; Murray, R. W. *J. Am. Chem. Soc.* **1978**, *100*, 7870.
(16) Martin, C. R.; Rubinstein, I.; Bard, A. J. *J. Am. Chem. Soc.* **1982**, *104*, 4817.
(17) Feldberg, S. W.; Rubinstein, I. *J. Electroanal. Chem.* **1988**, *240*, 1.
(18) (a) Goodwin, H. A.; Kepert, D. L.; Patrick, J. M.; Skelton, B. W.; White, A. H. *Aust. J. Chem.* **1984**, *37*, 1817. (b) Ferguson, J. E.; Love, J. L.; Robinson, W. T. *Inorg. Chem.* **1972**, *11*, 1662. (c) Rillema, D. P.; Jones, D. S.; Levy, H. A. *J. Chem. Soc., Chem. Commun.* **1979**, 849.
(19) Smith, C. P.; White, H. S. *Langmuir* **1993**, *9*, 1.
(20) Smith, C. P.; White, H. S. *Anal. Chem.* **1992**, *64*, 2398.
(21) Wightman, R. M.; Wipf, D. O. *Electroanalytical Chemistry*; Bard, A. J., Ed.; Marcel Dekker: New York, 1989; Vol. 15.

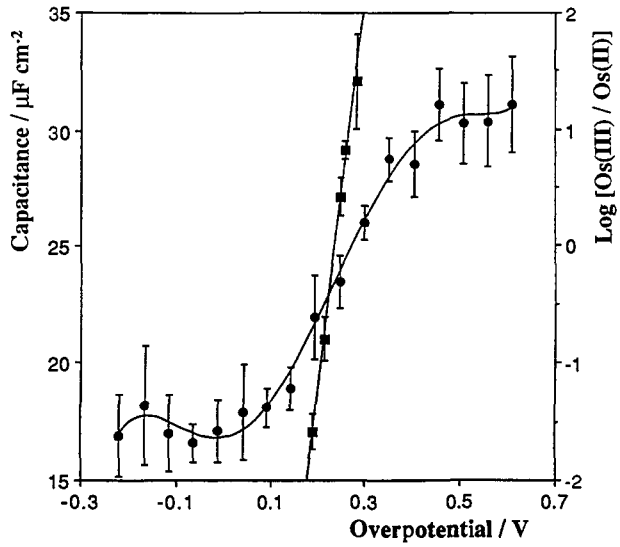

Figure 2. Double layer capacitance and redox composition as a function of potential for a p3p monolayer. The supporting electrolyte was aqueous 0.1 M $NaClO_4$. A solid circle denotes the capacitance data and a solid square denotes the log[Os(III)/Os(II)] ratio. The double layer capacitance was calculated using the microscopic electrode area.

capacitance observed for a reduced monolayer is at least two times smaller than the value observed for an unmodified electrode in the same electrolyte (40–50 $\mu F\ cm^{-2}$). This behavior is consistent with a compact monolayer being formed at the interface, at the expense of water and anion displacement. Figure 2 also shows that the interfacial capacitance depends on the redox composition, with the interfacial capacitance becoming larger as the film becomes increasingly oxidized. A higher dielectric constant at the interface, or a decrease in the distance of closest approach, is likely to be an important factor in determining the observed change. The movement of charge compensating counterions and probably solvent into the monolayer upon oxidation would probably cause the effective dielectric constant to increase and the distance of closest approach to decrease. Both of these effects would cause the interfacial capacitance to be higher for the oxidized film. However, we note that the layer of fixed charges near the electrode surface complicates the interpretation of capacitance data.

While we observe a significant reduction (>20%) in the interfacial capacitance for monolayers in $NaClO_4$, KNO_3, K_2SO_4, and NaCl compared with the unmodified interface, hydrophilic anions such as chloride give a higher interfacial capacitance than lipophilic anions such as perchlorate. This behavior suggests that the extent of ion pairing and solvent penetration across the monolayer/electrolyte interface depends on the identity of the anion in solution. Such a result is not entirely unexpected; it is known for example, that in the case of self-assembled monolayers of *N*-(*n*-decyl)-*N'*-(10-mercaptodecyl)-4,4'-bipyridinium dichloride, perchlorate is transported with almost no associated solvent, and that specific interactions exist between perchlorate and the positively charged viologen moieties.[22]

Ion Pairing Effects. The formal potential of the electroactive group is sensitive to both the solvation shell of the redox center and the extent of ion pairing and is therefore a sensitive probe of the local microenvironment within the monolayer.[23] Shifts in formal potential with changes in electrolyte concentration reflect differences in the relative stability between the two redox states and can be used to probe ionic interactions. Therefore, by examining the electrolyte activity dependence of $E^{\circ\prime}$, information about the extent of ion pairing can be obtained.[24,25]

We have determined $E^{\circ\prime}$ as a function of the supporting electrolyte concentration using cyclic voltammetry, where the solvent is water or THF. In order to minimize liquid junction potential effects and to increase the solution's conductivity, a fixed 1.0 M background of another salt was used as the concentration of the electrolyte of interest was changed from approximately 0.01 to 1.0 M. Potassium nitrate and tetrabutylammonium tetrafluoroborate were used, where the solvent was water and THF, respectively. If these salts are to act as swamping electrolytes, it is important that they exhibit little tendency to form ion pairs with the osmium redox centers. Consequently, we have confirmed in separate experiments that $E^{\circ\prime}$ changes by less than 15 mV as the concentration of these electrolytes is changed from 0.01 to 1.0 M.

In probing the electrolyte concentration dependence of $E^{\circ\prime}$, scan rates between 5 and 50 V/s were used, where the peak splitting between anodic and cathodic branches was independent of scan rate, indicating that the interfacial kinetics do not control the response. The peak shapes and heights do not change with electrolyte concentration, but $E^{\circ\prime}$ shifts progressively more negative as the electrolyte concentration increases. This negative shift indicates that oxidation of the redox center becomes thermodynamically more facile at high electrolyte concentrations and is consistent with ion pairing between the electrolyte anion and the redox centers. This situation is summarized in the following Nernstian reaction,

$$(pNp)^{+}(X^{-})_{\zeta} - e^{-} + p(X^{-}) \rightleftarrows (pNp)^{2+}(X^{-})_{\zeta+p}$$

where both redox forms are considered to participate in the ion pairing equilibria.

Plots of $E^{\circ\prime}$ vs the logarithm of the electrolyte concentration are linear for p0p monolayers in both tetrahydrofuran and water. The theoretical slopes of these plots are $(59/p)$ mV/decade, and we have used them to determine the difference in the number of ions that are paired with the redox center in its reduced and oxidized states. The slope in THF is 51 mV/decade, where the electrolyte is tetrabutylammonium perchlorate. This slope suggests that a single extra anion becomes paired with the redox center upon oxidation.[26] It is therefore likely that the reduced monolayer is ion paired with a single perchlorate anion, and that oxidation to the 2+ state causes a second perchlorate to become strongly bound. In contrast, the slope is only 24 mV/decade in aqueous perchlorate. This slope corresponds to $p = 2$ and suggests that $(pNp)^{+}$ monolayers are not ion paired but that two perchlorate anions are strongly bound to $(pNp)^{2+}$ monolayers. The observation that the extent of ion pairing is solvent dependent is important, and we explore its effect on the interfacial kinetics later.

To further probe the importance of ion association, we have determined fwhm in aqueous media for a p2p monolayer as a function of temperature, where the supporting electrolyte is perchlorate or nitrate, and Table 1 contains these data. In these experiments the integrated charge under the peaks remains constant with changing temperature, indicating the thermal stability of these monolayers throughout these experiments. Table 1 shows that where the supporting electrolyte is nitrate, the peak width increases from 100 to 114 mV as the temperature is increased from 5 to 40 °C. While these peak widths are somewhat larger than those ideally expected in the absence of lateral interactions (84–95 mV), the increase in peak width over this temperature range is consistent with thermal broadening. In sharp contrast, however, the peak width at 40 °C in perchlorate-containing media is considerably smaller than that at 5 °C. Laviron,[14a] as well as Brown and Anson,[14b] have considered the effect of lateral interactions between adsorbates on cyclic voltammetry. As the potential is scanned, the reduced (R) and oxidized (O) forms the redox couple coexist near $E^{\circ\prime}$. The peak

(22) DeLong, H. C.; Buttry, D. A. *Langmuir* **1990**, *6*, 1319.
(23) Creager, S. E.; Rowe, G. K. *Anal. Chim. Acta* **1991**, *246*, 233.
(24) Rowe, G. K.; Creager, S. E. *Langmuir* **1991**, *7*, 2307.
(25) (a) Nagamura, T.; Sakai, K. *Chem. Phys. Lett.* **1987**, *141*, 553. (b) Nagamura, T.; Sakai, K. *J. Chem. Soc., Faraday Trans.* **1988**, *84*, 3529.
(26) Buttry, D. A. *Langmuir* **1990**, *6*, 1319.

Table 1. Full Width at Half Maximum for Cyclic Voltammetry of p2p Monolayers vs Temperature[a]

	fwhm mV	
T,[b] °C	ClO_4^-	NO_3^-
40	95(3)	114(3)
35	98(4)	110(4)
30	102(4)	111(3)
25	105(3)	108(4)
20	107(2)	109(5)
15	111(4)	102(5)
10	113(4)	104(4)
5	118(5)	100(2)

[a] Numbers in parentheses represent the standard deviations for at least three individual monolayers. The solvent is water. [b] The temperature was controlled to within ±0.2 °C.

sharpening observed in aqueous perchlorate media with increasing temperature indicates increasingly attractive interactions between OR pairs. The observation that the peak width at 40 °C is 95 mV and agrees exactly with theory might suggest that the monolayer is ideal and that there is no ion pairing present. However, we have determined the concentration dependence of $E^{\circ\prime}$ at 40 °C and find that there is an extra anion paired with the oxidized state.

Reaction Entropies. There is no *a priori* reason to anticipate that the solvent cage of a redox center within a monolayer would be identical to that of a solution species. Indeed, one might suspect that both the solvent ordering and the effective dielectric constant would be different in the two circumstances. Solvent molecules within a monolayer can alter the thermodynamics of electron transfer in two distinct ways. Intercalated solvent can insulate the redox centers from adjacent repulsive electrostatic charges and can also influence the extent of ion pairing. Reduction of lateral electrostatic interactions will clearly be more efficient in media of high dielectric constant. In contrast, ion pairing resulting in partial neutralization of the polycationic monolayer is more pronounced in low dielectric media.

The reaction entropy ΔS_{rc}° quantifies the entropy difference between the reduced and oxidized forms of the redox couple and is expected to be dominated by differences in solvent and counterion ordering. We have determined the reaction entropy from the temperature dependence of the formal potential using a non-isothermal cell,[27,28]

$$\Delta S_{rc}^\circ = F(\partial E^{\circ\prime}/\partial T) \quad (2)$$

where F is the Faraday constant and T is the absolute temperature. Figure 3 shows the cyclic voltammetric response for a p0p monolayer as the temperature is changed from 37 to 7 °C, where the supporting electrolyte is aqueous 0.1 M $NaClO_4$. The formal potentials of these redox centers, either bound within monolayers or free in solution, always shift in a positive potential direction with increasing temperature. Plots of $E^{\circ\prime}$ vs T are linear, and the slopes provide reaction entropies. The positive shift in $E^{\circ\prime}$ with increasing temperature gives positive reaction entropies, indicating a higher degree of local ordering in the 3+ oxidation state. The dielectric continuum theory can provide an estimate of the reaction entropy via the Born equation,[29]

$$\Delta S_{rc}^\circ(\text{Born}) = -N_A \Delta e^2 (\partial \epsilon_s/\partial T)[(z_R + 1)^2 - z_R^2]/(2r\epsilon_s^2) \quad (3)$$

where N_A is Avogadro's constant, e is the electronic charge, ϵ_s is the static dielectric constant, z_R is the charge on the reduced form of the redox couple, and r is the radius of the complex (7.5 Å).[18] Figure 4 compares the experimentally determined reaction entropies for both the p2p monolayer and the model complex in solution with those calculated from the Born equation. The experimental monolayer data and theory are highly correlated, and a near unity slope is observed. The ability of the Born electrostatic model to approximately predict both the magnitude of the reaction entropy and the dependence on solvent dielectric character for the p2p system is certainly noteworthy. Figure 4 also includes the observed reaction entropies for the solution analog, $[Os(bpy)_2(pyridine)Cl]PF_6$. These data show that while there is a linear correlation between the experimentally determined ΔS_{rc}° and that predicted by the Born model, the slope is only about half that observed for the monolayer. The difference between the bound and free systems could be due to steric congestion in the monolayer, which may significantly inhibit complete insertion of charge compensating counterions, thus causing increased polarization around the redox center and a higher reaction entropy. It is also interesting to speculate as to the effect of the electric field in the two situations. In the case of the spontaneously adsorbed monolayer, the close-packed structure and perhaps a lower dielectric constant may cause a higher electric field strength to be experienced by the bound

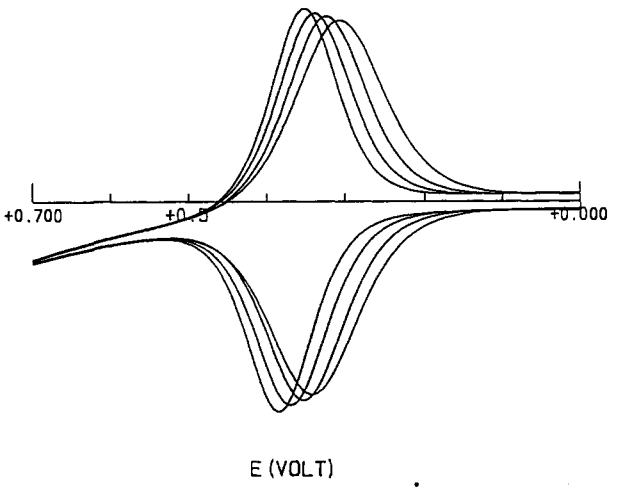

Figure 3. Effect of temperature on the cyclic voltammetry of a p0p monolayer in aqueous 0.1 M $NaClO_4$. The temperatures are, from left to right, 37, 25, 15, and 7 °C, respectively. The scan rate is 51 V/s. Both anodic and cathodic branches shift equally with changes in temperature.

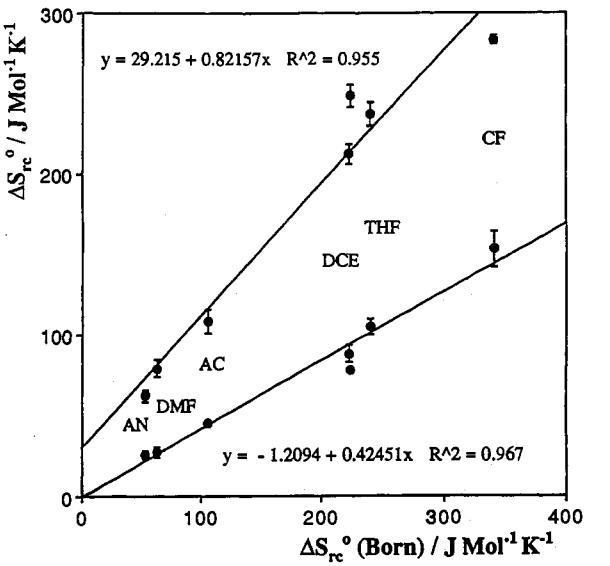

Figure 4. Correlation observed between the experimentally determined reaction entropy ΔS_{rc}° and that predicted by the Born dielectric continuum theory (eq 3) for p2p monolayers (top) and a solution-phase model compound, $[Os(bpy)_2(pyridine)Cl]PF_6$ (bottom). Data points for particular solvents lie immediately above and below the corresponding label. All solvents contained 0.1 M perchlorate as supporting electrolyte.

(27) Hupp, J. T.; Weaver, M. J. *J. Phys. Chem.* **1984**, *88*, 1860.
(28) Barr, S. W.; Guyer, K. L.; Li, T. T.-T.; Liu, H. Y.; Weaver, M. J. *J. Electrochem. Soc.* **1984**, *131*, 1626.
(29) Noyes, R. M. *J. Am. Chem. Soc.* **1962**, *84*, 513.

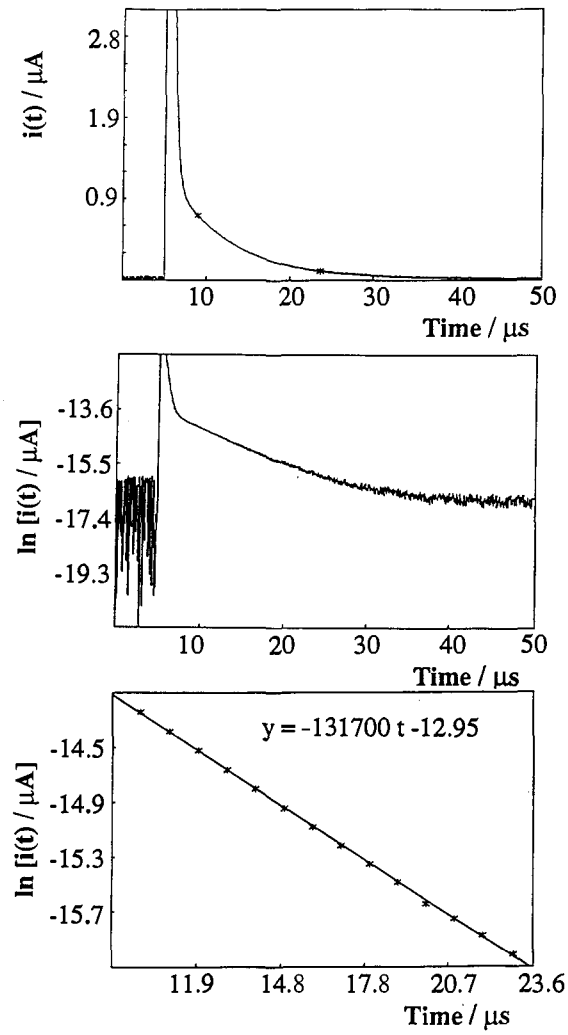

Figure 5. Current response of a 5 μm radius platinum microelectrode modified with a spontaneously adsorbed p3p monolayer following a potential step where the overpotential $[\eta = (E - E^{\circ\prime})]$ was −0.200 V. The supporting electrolyte is 0.1 M TEAP in DMF. The middle frame shows the first-order plot for data between the marks on the current–time transient in the upper frame. The time axis of the lower frame is referenced to the leading edge of the potential step.

centers.[30] This could induce greater solvent ordering causing a higher reaction entropy to be observed.

Chronoamperometry. Potential step chronoamperometry allows one to probe the uniformity of electron transfer rates, thereby testing the degree of order within the monolayer. For an ideal electrochemical reaction involving a surface-bound species, the Faradaic current following a potential step exhibits a single exponential decay in time,[30,31]

$$i_F = kQ \exp(-kt) \qquad (4)$$

where k is the apparent rate constant for a given overpotential, and Q is the total charge passed in the redox transformation.

Figure 5 illustrates an example of the chronoamperometric response observed for a p3p monolayer, where the electrolyte is 0.1 M TEAP in DMF. This response is typical of the three monolayers in all solvents examined. The semilog plot in Figure 5 shows that on a microsecond time domain two current decays can be time resolved. These responses, which arise from double layer charging and Faradaic current flow, are time resolved due to the much shorter RC time constant of double-layer charging compared to that of the Faradaic reaction. In our investigations we have restricted the determination of the electron transfer rate constant to those situations where the time constant of double-layer charging is at least 5 times shorter than the time constant of the Faradaic reaction. Electron transfer appears to be characterized by a single rate constant over the time required to collect greater than 95% of the Faradaic charge. Different portions of the Faradaic transient were analyzed to test the kinetic homogeneity of the redox centers and to determine if other nonexponential current contributions were present. The monolayers always gave linear first-order decays over about 2 lifetimes. Further evidence suggesting the predominance of a single rate constant is obtained by examining the intercept of the first-order plot at zero time (lower frame, Figure 5). As indicated in eq 4, the intercept for a single exponential decay is ln (kQ). This chronoamperometric determination of the charge passed can then be compared with the value determined using cyclic voltammetry in order to further test the ideality of the chronoamperometric response. We find that the charges passed in these two independent experiments agree to within 5–10%.

The observation of a single interfacial rate constant suggests that the local microenvironments of the individual redox centers are all similar, or that there is rapid interconvertibility. However, if interconversion of dissimilar sites occurs, it is a short time scale phenomenon that makes all redox sites actively undergoing electron transfer chemically identical. In this sense, the measured rate constants would be representative of an average adsorbed molecule undergoing electron transfer. Our data do not give an insight into the structure that precedes or follows electron transfer. Deviations from linearity would be expected if kinetic dispersion or iR drop were present. Uncompensated resistance acts to weaken the potential experienced by the redox centers and causes the potential, and hence the apparent rate, to evolve with time.[30] Therefore, iR drop would produce negative deviations in the observed current at short times. In order to test the possibility that counterion availability, or double-layer effects, influence the heterogeneous electron transfer reaction, we have determined the standard heterogeneous rate constant k° in several solvents as a function of the electrolyte concentration. Table 2 shows how the interfacial rate constant depends on perchlorate concentration for a p3p monolayer, where the solvents are water, acetonitrile, and dimethylformamide. These data show that the inter-monolayer precision on k° is approximately 5%, reflecting a highly reproducible monolayer structure. Importantly, Table 2 also shows that the mean value of k° increases by only about 20% as the perchlorate concentration is increased from 0.1 to 1.0 M. The observation that the electrode kinetics are approximately independent of the electrolyte concentration suggests that ion pairing does not directly influence the electron transfer process over the concentration range of interest and that diffusion/migration of charge-compensating counterions is not the rate determining step. However, we recognize that a saturated ion-pairing condition may be achieved even in 0.1 M perchlorate. Table 2 suggests that iR drop and double-layer effects on the interfacial kinetics are negligible. These observations suggest that chronoamperometry measures elementary electron transfer rates. These data

Table 2. Dependence of the Standard Heterogeneous Rate Constant k^0 for p3p Monolayers on the Supporting Electrolyte Concentration and the Solvent[a]

electrolyte concn M	$10^{-4}k^0(H_2O)$,[b] s^{-1}	$10^{-4}k^0(AN)$,[c] s^{-1}	$10^{-3}k^0(DMF)$,[c] s^{-1}
0.1	6.31(0.26)	1.80(0.06)	3.51(0.08)
0.2	6.34(0.16)	1.82(0.09)	3.63(0.07)
0.4	6.73(0.30)	1.84(0.07)	3.81(0.15)
0.6	6.82(0.19)	1.92(0.09)	3.95(0.10)
0.8	7.11(0.27)	2.08(0.08)	4.04(0.20)
1.0	7.27(0.24)	2.09(0.10)	4.18(0.18)

[a] Inter-monolayer standard deviations ($n \geq 3$) are in parentheses. All standard rate constants were determined at 298 K. [b] Supporting electrolyte is $NaClO_4$. [c] Supporting electrolyte is tetraethylammonium perchlorate (TEAP).

(30) Bard, A. J.; Faulkner, L. R. *Electrochemical Methods: Fundamentals and Applications*; Wiley: New York, 1980.
(31) Finklea, H. O.; Hanshew, D. D. *J. Am. Chem. Soc.* **1992**, *114*, 3173.

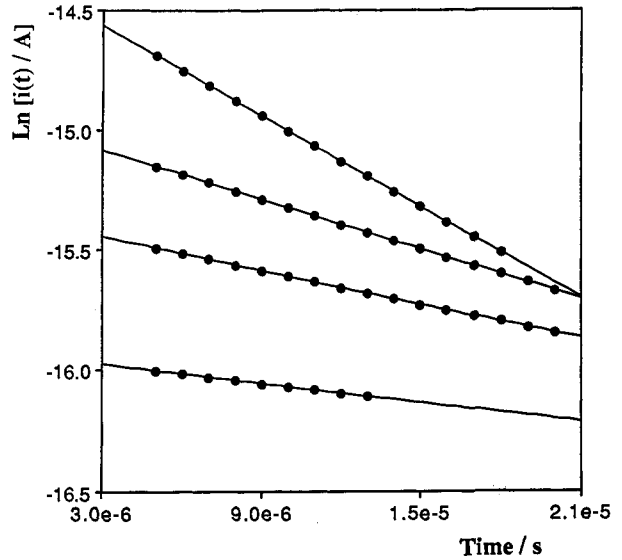

Figure 6. Effect of various overpotentials (η) on the ln $i(t)$ vs t plots for a spontaneously adsorbed p3p monolayer. The supporting electrolyte was 0.1 M TEAP in DMF. Taken on the left-hand side, the overpotentials are from top to bottom, 0.203, 0.152, 0.102, and 0.070 V, respectively.

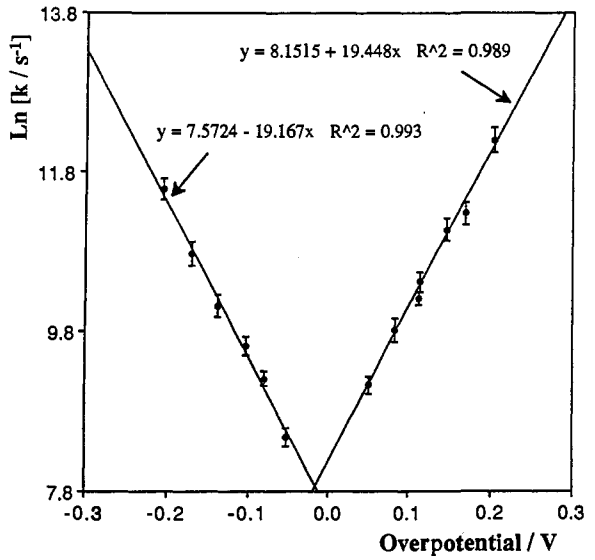

Figure 7. Dependence of ln k on the overpotential for a spontaneously adsorbed p3p monolayer. The supporting electrolyte is 0.1 M TEAP in DMF. Data were collected using a 25 μm radius microelectrode.

also show that $k°$ depends markedly on the nature of the electrochemical solvent, and we explore the origin of this effect in detail in the following paper.[8]

Potential Dependence of k. In an amperometric experiment, an increased step potential relative to $E°'$ increases the free energy driving force for the reaction and causes increased electron transfer rates to be observed.[30] Figure 6 illustrates the effect of various overpotentials ($\eta \equiv E - E°'$) on the ln $i(t)$ vs t plots observed for p3p monolayers, where the electrolyte is 0.1 M TEAP in DMF. This figure shows that both the slope $-k$ and intercept ln (kQ) are dependent on the overpotential. A semilog plot (Tafel plot) of the measured rate constants at 25 °C vs the overpotential is given in Figure 7. The linear response and slopes observed are consistent with the Butler–Volmer formulation of the potential dependence of electrochemical reaction rates.[30] However, this figure shows that specifying the overpotential with respect to the cyclic voltammetric formal potential gives forward and backward rate constants that are not equal for $\eta = 0$. Determining the overpotential relative to the cyclic voltammetric formal potential yields "standard" rate constants of 3.5×10^3 and 1.9×10^3 s^{-1} for the oxidation and reduction processes, respectively. Figure 7 suggests that the effective formal potential in short time scale chronoamperometry (i.e. the potential where the forward and backward rate constants are equal) is shifted by approximately −15 mV compared to the cyclic voltammetric value. This is a general feature of the monolayers, and the magnitude of the shift is larger in low dielectric constants, e.g., in tetrahydrofuran, the apparent chronoamperometric formal potential is shifted by approximately −46 mV.

Scheme 1

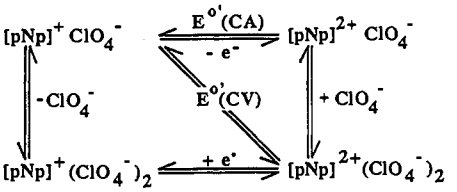

Table 3. Dependence of the Standard Heterogeneous Rate Constant ($k°$) and Tunneling Parameter ($\beta°$) on the Solvent for p0p, p2p, and p3p Monolayers[a]

solvent	$10^{-4}k°$(p0p), s^{-1}	$10^{-4}k°$(p2p), s^{-1}	$10^{-4}k°$(p3p), s^{-1}	$\beta°$, Å^{-1}
AN	>70	11.0(0.3)	1.80(0.08)	1.8
AC	>70	6.43(0.15)	1.36(0.04)	1.6
DMF	55(4)	1.77(0.05)	0.35(0.01)	1.6
THF	37(3)	1.05(0.03)	0.21(0.01)	1.6
DCE	22(2)	0.95(0.03)	0.20(0.02)	1.5
CF	19(1)	0.72(0.04)	0.161(0.004)	1.5

[a] Inter-monolayer standard deviations ($n \geq 3$) are in parentheses. All standard rate constants were determined at 298 K. The values are given by the crossing point of the extrapolated anodic and cathodic branches of the Tafel plot at low η (<200 mV). AN is acetonitrile, AC is acetone, DMF is dimethylformamide, THF is tetrahydrofuran, DCE is dichloroethane, and CF is chloroform. The supporting electrolyte concentration is 0.1 M perchlorate.

The origin of this shift may lie in the ion-pairing effects we discussed earlier. Ion association–dissociation may cause the effective cyclic voltammetric (long time scale) and chronoamperometric (short time scale) formal potentials to be different. It is possible, for example, that the cyclic voltammetric $E°'$ reflects a fully-ion-paired situation, while the short time scale of chronoamperometry does not allow sufficient time for association between the oxidized redox center and the perchlorate anion to occur fully. This situation is summarized in Scheme 1. The identity of the charge compensating species may also depend on the experimental time scale.[32]

The oxidation state of the film changes throughout the Faradaic current decay induced by stepping the potential. For example, in the experiment illustrated in Figure 5, the monolayer is initially fully oxidized, and over the 50 μs following the potential step, its macroscopic oxidation state evolves to give a fully reduced film. Therefore, the observation of a time-independent reaction probability (Figures 5 and 6) suggests that the monolayer conformation is not a function of the macroscopic oxidation state of the monolayer. Thus one can effectively exclude distinct conformations of the monolayer, in the oxidized and reduced states, from being responsible for the observed differences in the standard rate constants suggested by Figure 7. The absence of conformational effects on k agrees with molecular dynamics simulations of monolayers, which suggest that conformational changes occur on a nanosecond time scale.[33]

Tunneling Mechanism. As shown in Table 3, the rate of electron transfer is relatively slower in chloroform. In the following paper, we show that this reduced rate mirrors the slow rate at which chloroform can relax dielectrically to accommodate the new charge on the monolayer after redox switching. The relatively slower interfacial kinetics allows us to probe the kinetics over a large range of driving force. Figure 8 illustrates Tafel plots for p2p

(32) Mąjda, M.; Faulkner, L. R. *J. Electroanal. Chem.* **1984**, *169*, 77.
(33) Hautman, J.; Klein, M. L. *J. Chem. Phys.* **1989**, *91*, 4994.

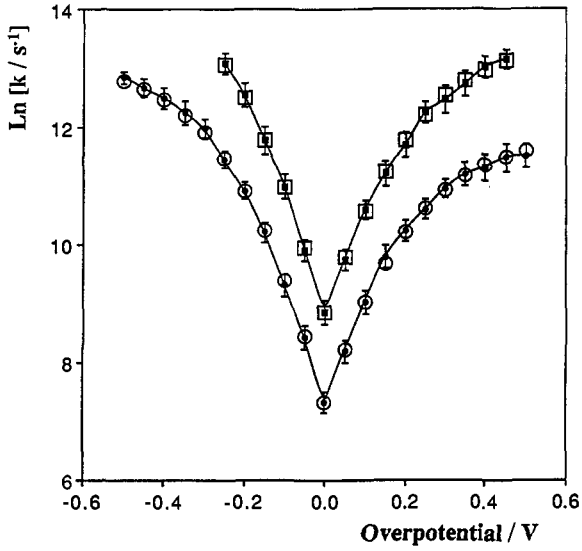

Figure 8. Tafel plot for p2p and p3p monolayers where the supporting electrolyte is 0.1 M TBAP in chloroform. Solid squares (top) and circles (bottom) denote the p2p and p3p experimental data, respectively. Open squares and circles denote the fitted data from eq 5–8 where β is held constant at 1.5 Å^{-1} and λ equals 27.7 and 26.4 kJ mol^{-1} for the p2p and p3p monolayers, respectively.

and p3p monolayers where the solvent is chloroform. The dependence of ln k on η is clearly nonlinear at large overpotentials, and the slopes decrese in magnitude with increasing overpotential in both anodic and cathodic directions. In the conventional Butler–Volmer formulation of electrode kinetics,[30] for a one-electron process the slope magnitudes are $\alpha_c F/RT$ and $\alpha_a F/RT$ for the reduction and oxidation reactions, respectively. Therefore, Figure 8 suggests that the transfer coefficients are potential dependent. Furthermore, the data are asymmetric with respect to overpotential, with α_a tending toward zero more rapidly than α_c. Double-layer effects or imperfections within the monolayer could account for the observed curvature. However, the first-order plots remain linear at high overpotentials, suggesting that the monolayer structure is homogeneous. Also, as discussed previously, k is approximately independent of electrolyte concentration, suggesting that the time required to assemble the double layer is not important.

Nonlinear Tafel plots are expected on the basis of Marcus theory due to the presence of a term that is quadratic in η in the rate equation.[34] Simplified models of electron tunneling based on the Marcus theory have been developed for monolayers.[31,35,36] However, published theory describing through-bond tunneling does not predict the observed asymmetry in the Tafel plot shown in Figure 8. Finklea and Hanshew[31] have assembled a model describing through-space electron tunneling which does allow for the asymmetry. In this model the cathodic rate constant is given by integral over energy ($\mathcal{E}$) of three functions: (a) the Fermi function for the metal, $n(\mathcal{E})$; (b) a Gaussian distribution of energy levels for acceptor states in the monolayer, $D_{Ox}(\mathcal{E})$; and (c) a rate parameter for electron tunneling at a given energy, $p(\mathcal{E})$.

$$k = \mathcal{A}\int_{-\infty}^{\infty} n(\mathcal{E})\, D_{Ox}(\mathcal{E})\, p(\mathcal{E})\, d\mathcal{E} \qquad (5)$$

The zero point of energy is defined as the Fermi level of the metal at the particular overpotential of interest. The Fermi function describes the distribution of occupied states within the metal and is defined by

$$n(\mathcal{E}) = [1 + \exp(\mathcal{E}/k_B T)]^{-1} \qquad (6)$$

where k_B is the Boltzmann constant. The density of acceptor states is derived from the Marcus theory[34,37] and is represented by eq 7,

$$D_{Ox}(\mathcal{E}) = \Gamma(4\pi\lambda k_B T)^{-1/2} \exp[-(\mathcal{E} - \lambda - e\eta)^2/(4\lambda k_B T)] \qquad (7)$$

where λ is the reorganization energy. Schmickler and co-workers treated the effect of tunneling through an energy barrier in conjunction with the Marcus model.[38] The probability of direct elastic tunneling[39] through a trapezoidal energy barrier of height $\mathcal{E}_B$ can be approximately by eq 8,

$$p(\mathcal{E}) = (\mathcal{E}_B - \mathcal{E} + e\eta/2) \exp(-\beta d) \qquad (8)$$

where $\mathcal{E}_B$ is the average barrier height at zero overpotential and d is the electron transfer distance.

The rate of electron tunneling decreases exponentially with increasing distance[6,31,40–42] and is controlled by the tunneling parameter β. For example, the standard rate constant would relate to the tunneling parameter obtained at the formal potential $\beta°$ as follows:

$$k° = k' \exp(-\beta° d) \qquad (9)$$

In the model assembled by Finklea and Hanshew,[31] β depends on the potential. However, there have been several experimental and theoretical reports suggesting that β is independent of the potential.[42,43] For our monolayers, we find (vide supra) that the potential dependence of the rate constant can be accurately modeled using a single reorganization energy for both anodic and cathodic branches, if β is fixed throughout the integration at the value experimentally determined at $E°'$.

At zero overpotential, the average barrier height is essentially identical to that predicted by classical tunneling theory[31,39b] and is defined by

$$\mathcal{E}_B = (9.48\beta°)^2 \qquad (10)$$

where $\mathcal{E}_B$ is in kJ mol^{-1} and $\beta°$ is in Å^{-1}.

The anodic rate constant is obtained by replacing $n(\mathcal{E})$ with its compliment, $1 - n(\mathcal{E})$, and substituting D_{Ox} with D_{Red}, in which $-\lambda$ is replaced with $+\lambda$.

A more negative potential elevates the pre-exponential in eq 8, so that the cathodic rate constants are larger than their anodic counterparts for a given absolute overpotential. Therefore, this not only predicts the curvature in Tafel plots but also can describe the asymmetry between cathodic and anodic rate constants shown in Figure 8. The model contains three unknowns, the pre-integral constant $\varkappa$, the reorganization energy λ, and the average barrier height $\mathcal{E}_B$.

We have used the experimentally determined $\beta°$ for chloroform (1.5 Å^{-1}) in conjunction with eq 10 to obtain a value of 202 kJ mol^{-1} for the average barrier height. This is similar to the barrier observed when a tunneling junction is formed using Langmuir–Blodgett monolayers of fatty acids between two metals.[44]

Having experimentally determined the average barrier height, there are only two freely adjustable parameters in eq 6–8, namely the pre-integral factor $\varkappa$ and the reorganization parameter λ. The reorganization parameter is intrinsic to the local

(34) Marcus, R. A. *J. Chem. Phys.* **1956**, *24*, 966.
(35) Finklea, H. O.; Ravencroft, M. S.; Snider, D. A. *Langmuir* **1993**, *9*, 223.
(36) Chidsey, C. E. D. *Science* **1991**, *251*, 919.
(37) Marcus, R. A. *J. Phys. Chem.* **1963**, *67*, 853.
(38) (a) Schmickler, W. *J. Electroanal. Chem.* **1977**, *82*, 65. (b) Schmickler, W.; Ulstrup, J. *J. Chem. Phys.* **1977**, *19*, 217.
(39) (a) Simmons, J. G. *J. Appl. Phys.* **1963**, *34*, 1793. (b) Bockris, J. O'M.; Khan, S. U. M. *Quantum Electrochemistry*; Plenum Press: New York, 1979; Chapter 8.
(40) Miller, C.; Cuendet, P.; Grätzel, M. *J. Phys. Chem.* **1991**, *95*, 877.
(41) Miller, C.; Grätzel, M. *J. Phys. Chem.* **1991**, *95*, 5225.
(42) Becka, A. M.; Miller, C. *J. Phys. Chem.* **1992**, *96*, 2657.
(43) Xu, J.; Li, H.-L.; Zhang, Y. *J. Phys. Chem.* **1993**, *97*, 11497.
(44) Mann, B.; Kuhn, H. *J. Appl. Phys.* **1971**, *42*, 4398.

microenvironment of the redox center, while the pre-factor depends on the extent of overlap between the metallic states of the electrode and the orbitals of the redox center. We have numerically integrated eq 5 to obtain theoretical rate constants under all conditions experimentally investigated. The reorganization parameter was chosen so that there was satisfactory agreement between shapes of the theoretical and the experimental results along the branches of the Tafel plot; then $\varkappa$ was adjusted to give the experimental $k°$. Figure 8 shows the experimental data together with the best fits provided by this model where $\lambda = 27.7$ and 26.4 kJ mol^{-1} for the p2p and p3p monolayers, respectively. These values are identical within experimental error.

The Marcus theory[34,37] can be used to calculate the reorganization energy. In this model, λ is considered to be the sum of an inner-sphere and an outer-sphere component. The inner-sphere component describes the distortion of bond angles and lengths accompanying electron transfer, while the outer-sphere component reflects solvent reorganization effects, the activation barrier for which is given by

$$\lambda = (\Delta e^2/2)(r^{-1} - R_e^{-1})(\epsilon_{op}^{-1} - \epsilon_s^{-1}) \qquad (11)$$

where R_e is the reactant–image distance. In the past, stabilizing reactant–image interactions have either been neglected for electrochemical reactions,[45] i.e., $R_e \rightarrow \infty$, or the reactant–image distance has been assumed to be twice the reactant–electrode separation. When compared with solution-phase reactants, imaging effects are likely to be less important for the long range electron transfer reactions investigated here, because the redox center is remote from the electrode surface. Therefore, we have neglected imaging effects in calculating λ as a function of the solvent. These values decrease by less than 25% if R_e is defined as twice the electrode–reactant separation. Equation 11 yields a reorganization energy of 25.5 kJ mol^{-1}, which agrees rather well with the average value of 27 ± 0.7 kJ mol^{-1} obtained from fitting the data in Figure 8. It is important to emphasize that the very satisfactory fit shown in Figure 8 is obtained using essentially the Marcus reorganization energy for both branches and both monolayers. Thus, no adjustable parameters are needed to predict the shape of the plot. The agreement between the theoretical λ value and those determined experimentally suggests that solvent reorganization is the dominant component in the activation barrier for electron transfer. We consider this aspect of the electron transfer mechanism in detail in the following paper.

We have determined $\beta°$ from the distance dependence of the standard rate constant, $k°$. A rigid rod model of the bridging ligands[46] suggests that the bridging ligand lengths are approximately 6.8, 9, and 10 Å for the p0p, p2p, and p3p monolayers, respectively. Although we recognize that this is a limited range, the standard rate constants given in Table 3 are consistent with eq 10 and give a $\beta°$ value of 1.6 ± 0.2 Å^{-1} for all solvents examined. The magnitude of $\beta°$ determined here is consistent with the value expected for through-space tunneling (1.3–1.8 Å^{-1})[27] and is considerably larger than values associated with through-bond tunneling.[31,35,47] The suggestion in our case of a through-space, rather than a through-bond, electron tunneling mechanism is somewhat unexpected and may be important. One might have anticipated that the aromatic character of our bridging ligands would have enhanced a through-bond tunneling process when compared with the alkanethiol monolayers. However, it is important to note that the electron transfer distances examined here (7–10 Å) are considerably shorter than those traditionally explored using alkanethiol self-assembled monolayers (20–30 Å).[48] Quantum mechanical spillover of the metal electron density beyond the electrode/monolayer interface and the delocalized character of the electron density on the electrode may be relatively more important for these short bridging ligands. Furthermore, the electric field strength is likely to be significant at 7 Å, and it may affect the elementary electron transfer event itself or associated processes.

Conclusions

Our attempts to diagnose the precise electron transfer mechanism are necessarily complicated by using theoretical models to interpret the experimental results. However, despite questions of interpretation and appropriate models, one can draw a number of important conclusions directly from the experimental observations. The nearly ideal cyclic voltammetry and chronoamperometry suggest that the electron transfer is mechanistically uncomplicated. Furthermore, the observation that semilog current vs time plots are always linear clearly demonstrates that electron transfer is a first-order process and tends to rule out bimolecular hopping between adjacent sites as a mechanism for switching the redox state of the monolayer. Lateral electron transfer would be expected to give diffusional responses characterized by a $t^{-1/2}$ dependency, if the active sites for heterogeneous electron transfer were widely spaced. If the active sites were more common and closer together the time dependency would be more complicated. The extent of ion pairing between the oxidized redox center and perchlorate anions depends on the electrochemical solvent. At equilibrium, the systems are apparently fully ion paired in both reduced and oxidized forms in low dielectric media. Greater solvent ordering occurs in all solvents when the monolayer is oxidized, but the entropy difference between reduced and oxidized forms is considerably larger in low dielectric media.

Experimentally, we observe that the logarithm of the rate constant increases linearly with increasing overpotential for overpotentials less than 200 mV. The transfer coefficients for both oxidation and reduction are indistinguishable from the value of 0.5 expected for a simple reversible reaction. These results agree with the predictions of the Butler–Volmer formulation of electrode kinetics. The curvature observed at high overpotentials is anticipated, since the Butler–Volmer approach is only a low driving force limiting case of the Marcus theory. The curvature experimentally observed is in excellent agreement with that predicted by the Marcus theory for simple outer-sphere reorganization. We observe a higher cathodic than anodic rate constant for a given absolute overpotential, which an existing electron transfer model predicts for a through-space tunneling mechanism. The tunneling parameter experimentally determined (1.6 ± 0.2 Å^{-1}) is considerably larger than the values associated with through-bond tunneling involving saturated hydrocarbon chains (0.8 Å^{-1}). Electron tunneling through the surrounding medium, rather than through the bridging ligand between the electrode and the redox center, ought to be sensitive to the surrounding solvent. Therefore, we consider the influence of static and dynamic solvent effects in the following paper.

Acknowledgment. We gratefully acknowledge the financial support of the National Science Foundation under Grant CHE-86-07984 and the Defense Advanced Research Projects Agency (via the office of Naval Research and subcontract from the Massachusetts Institute of Technology).

(45) Dzhavakhidze, P. G.; Kornyshev, A. A.; Krishtalik, L. I. *J. Electroanal. Chem.* **1987**, *228*, 329.
(46) Ghesquiere, D.; Ban, B.; Chachaty, C. *Macromolecules* **1977**, *10*, 743.
(47) Beratan, D. N.; Hopfield, J. J. *J. Am. Chem. Soc.* **1984**, *106*, 1584.
(48) Chidsey, C. E. D.; Bertozzi, C. R.; Putvinski, T. M.; Mujsce, A. M. *J. Am. Chem. Soc.* **1990**, *112*, 4301.